Am J Clin Exp Immunol 2026;15(5):372-382
www.ajcei.us /ISSN:2164-7712/AJCEI0169536

Original Article

Cyclophosphamide modulates renal GSK-3β and NF-κB p65 expression in MRL/lpr mice with lupus nephritis

Liuna Liang[1*], Zhian Yang[2*], Ying Chen[1], Ningning Gong[1], Linzhu Li[3], Haoling Zhang[4], Shuhong Zhou[1,5,6]

[1]Department of Immunology and Rheumatology, Gansu Provincial Hospital, Lanzhou 730000, Gansu, China; [2]Department of Respiratory Medicine, Gansu Provincial Hospital, Lanzhou 730000, Gansu, China; [3]Clinical College of Traditional Chinese Medicine, Gansu University of Chinese Medicine, Lanzhou 730000, Gansu, China; [4]Department of Biomedical Science, Universiti Sains Malaysia, Pinang 13200, Malaysia; [5]First School of Clinical Medical, Gansu University of Chinese Medicine, Lanzhou 730000, Gansu, China; [6]The Third Clinical Medical College of Lanzhou University, Lanzhou 730000, Gansu, China. [*]Equal contributors.

Received October 24, 2025; Accepted October 11, 2026; Epub October 25, 2026; Published October 30, 2026

Abstract: Lupus nephritis (LN) is a renal manifestation of systemic lupus erythematosus (SLE) in which immune-complex deposition and inflammation can result in renal tissue damage. The expression of GSK-3β and NF-κB p65 was analyzed in MRL/lpr mice during the development of LN and after cyclophosphamide (CTX) administration. Methods: In the longitudinal component, MRL/lpr and C57BL/6 mice were assessed at 12, 16, 20, 24, and 28 weeks of age (n=5 per group). A total of 10 MRL/lpr mice were assigned to untreated LN and CTX treatment intervention cohorts, with five C57BL/6 mice serving as controls. Starting at week 16, intraperitoneal CTX was given once a week, while LN and C57 mice were given saline. Serum, urine, and renal tissue were collected for ELISA, RT-qPCR, Western blotting, and pathological assessment at the end of 12 weeks. Results: Across the age series, MRL/lpr mice had greater urinary protein excretion, higher ANA and dsDNA concentrations, and worsening renal morphology with immune-complex deposition. Renal GSK-3β and NF-κB p65 expression also increased ($P < 0.05$). CTX did not significantly change 24-hour urinary protein excretion, but it was accompanied by lower ANA and dsDNA concentrations, less severe renal pathological changes and immune-complex deposition, and reduced renal GSK-3β and NF-κB p65 gene and protein expression ($P < 0.05$). Conclusion: These observations place the GSK-3β/NF-κB p65 axis alongside the inflammatory phenotype and CTX response in this model; they do not establish a direct causal pathway. Whether CTX changes this pathway directly, or whether the expression pattern follows improvement in the renal inflammatory environment, requires dedicated intervention experiments.

Keywords: Lupus nephritis, GSK-3β, NF-κB p65, MRL/lpr mice, cyclophosphamide

Introduction

Loss of immune tolerance can lead to systemic lupus erythematosus (SLE) by enabling autoantibody production and the formation of circulating antigen-antibody complexes. Widespread deposition of immune complexes in target organs contributes to the heterogeneous tissue injury seen in SLE [1]. Renal involvement is common: 25% to 60% of patients with SLE develop LN within five years, with roughly one in ten affected patients progressing to end-stage renal disease (ESRD) over the subsequent decade [2, 3]. The reported 10- and 20-year survival is approximately 70% and 60%, respectively [4]. Therefore, markers of both systemic immune activity and local renal damage may be necessary to complement routine clinical assessment and to follow changes in disease activity over time. A useful marker panel should therefore be interpreted across clinical, serological, and renal-tissue domains, because no single measurement can represent every feature of LN.

NF-κB p65 provides inflammatory transcriptional signaling that is detectable in activated B lymphocytes from patients with lupus and has been associated with LN outcomes [5]. In renal mesangial cells, increased NF-κB activity accompanies matrix remodeling and greater production of pro-inflammatory cytokines. GSK-3β,

a serine/threonine kinase linked to Wnt regulation, can intersect with these inflammatory processes. Considering the two molecules together may therefore help relate immune dysregulation to glomerular and tubulointerstitial injury in LN. This rationale does not require the two proteins to have identical roles; rather, it supports their parallel assessment within the inflammatory environment of the diseased kidney.

Experimental studies suggest that GSK-3β can promote NF-κB activation and downstream inflammatory signaling [6]. It has also been linked to pathogenic Th17-cell differentiation [7] and, in MRL/lpr mice, to anti-dsDNA autoantibody production and glomerulonephritis [8]. Even so, its renal expression pattern across LN progression and its relationship with treatment-associated changes remain insufficiently characterized. Mapping those patterns was therefore a central aim of the present work. The focus was on observed expression changes in renal tissue, with serological and pathological results providing the context for their interpretation.

Cyclophosphamide (CTX) is still used for severe or active LN, and conventional CTX-containing regimens have been associated with better renal survival than glucocorticoids alone [9]. The downstream events that accompany its renal effects, however, are not fully resolved. Renal inflammatory signaling was consequently examined here as a treatment-associated outcome rather than assumed to be a proven drug target. This distinction guided both the reporting of the intervention findings and the cautious interpretation of their potential mechanisms.

We first used the age series to identify an appropriate intervention stage in MRL/lpr mice. The subsequent 12-week CTX experiment compared renal GSK-3β and NF-κB p65 expression with serological and pathological findings. The design was intended to describe concurrent changes during LN and after treatment, not to test direct molecular causation.

Materials and methods

Experimental animals and LN model establishment

Experiments were performed with thirty-five 4-week-old female MRL/lpr mice as the experimental group and thirty age-matched female C57BL/6 mice as genetic controls. MRL/lpr mice were purchased from Cavens Biogle (Suzhou) Model Animal Research Co., Ltd., and C57BL/6 mice were supplied by the Experimental Animal Center of Gansu University of Chinese Medicine. All animals were maintained under specific pathogen-free conditions.

In the time-course experiment, MRL/lpr and C57BL/6 mice were randomly grouped (n=5 per group) and assessed for LN progression at 12, 16, 20, 24, or 28 weeks of age. At each time point, pathological findings and molecular expression levels were compared with those in age-matched C57BL/6 controls.

Ten MRL/lpr mice were randomly assigned to either the LN or LN-CTX group, and five C57BL/6 mice served as normal controls in this pharmacological study. To prepare the CTX solution, 200 mg of dry powder was dissolved in 2 mL saline and then diluted with 198 mL saline. From 16 weeks of age, the LN-CTX group received weekly intraperitoneal CTX injections at 80 mg/kg [dose (mg) = body weight (kg) × 80 mg/kg; Cat. No. C106991, purity ≥ 97%, Aladdin, Shanghai, China] [10]. The LN and C57 groups received equal volumes of saline on the same schedule for 12 weeks. The dose was calculated from each animal's body weight according to the stated formula.

At the end of the protocol, mice were euthanized by administration of intraperitoneal sodium pentobarbital. Serum, urine, and kidney tissues were collected and stored for subsequent analyses. Histology-designated kidney samples were fixed in 10% neutral buffered formalin, and the remaining tissues were stored at low temperature for molecular assays. Histological evaluation utilized fixed tissue, while the remaining stored specimens were used for the molecular assessments described below. The study was approved by the Medical Ethics Committee of Gansu Provincial People's Hospital (Approval No. 2020-169) and followed ARRIVE guidelines.

Measurement of 24-hour urinary protein

Urine was collected from all mice over a 24-h duration. Urinary protein concentration was measured with a biochemical analyzer in accor-

dance with the manufacturer's instructions and interpreted together with the urine volume collected over the same time frame. Note that this provided an integrated measure of the amount of protein excreted rather than a single spot-urine measurement.

Enzyme-linked immunosorbent assay (ELISA)

Serum ANA and dsDNA concentrations, as well as serum and urinary GSK-3β and NF-κB p65 concentrations, were determined with ELISA kits according to the manufacturers' instructions. The absorbance was measured at 450 nm with a microplate reader, and the concentrations were calculated from their corresponding standard curves. This assay measured GSK-3β and NF-κB p65 levels in the two biological sample types collected for the study.

Histopathological examination and immunofluorescence analysis

Kidney tissue was fixed, paraffin-embedded, sectioned, and stained with hematoxylin and eosin (HE), periodic acid-silver methenamine (PASM), and Masson stain to evaluate renal lesions, glomerular injury, and fibrosis. The combined staining approach allowed the evaluation to consider glomerular changes, interstitial abnormalities, and fibrotic features within the same renal specimens.

For immunofluorescence, frozen renal sections were incubated with antibodies against immunoglobulin A (IgA), IgG, IgM, complement component 1q (C1q), and C3 to assess renal immune-complex deposition. Fluorescence images were acquired for evaluation. Signal distribution and relative intensity were used to compare immune-complex deposition among groups.

Reverse transcription real-time quantitative polymerase chain reaction (RT-qPCR)

Total RNA was extracted from the renal cortex using TRIzol reagent. RNA concentration and purity were assessed with a nucleic acid analyzer, and qualified samples were reverse transcribed to complementary DNA (cDNA). Quantitative PCR was performed with GoTaq qPCR Master Mix (**Table 1**). Relative GSK-3β and NF-κB p65 expression was calculated by the comparative Ct method. Only RNA samples that met the concentration and purity assessment criteria were carried forward to reverse transcription and quantitative analysis.

Western blotting (WB) analysis

Total protein was isolated from renal tissue with RIPA lysis buffer containing PMSF, and protein concentration was determined by a BCA assay. Equal protein amounts were separated by SDS-PAGE, transferred to PVDF membranes, and incubated with the relevant primary and secondary antibodies. Signals were visualized by enhanced chemiluminescence, and GSK-3β and NF-κB p65 expression was evaluated. The protein data were considered together with the corresponding RT-qPCR measurements when describing renal expression changes.

Immunohistochemistry (IHC)

Paraffin-embedded kidney sections underwent antigen retrieval, endogenous peroxidase blocking, antibody incubation, and DAB visualization. GSK-3β and NF-κB p65 immunostaining was evaluated semi-quantitatively from staining intensity and the proportion of positive cells. The immunoreactivity score was calculated as staining intensity multiplied by the percentage of positive cells. This scoring method integrated the extent and strength of immunoreactivity when comparing renal regions across groups.

Statistical analysis

Normally distributed data are presented as the mean ± standard deviation ($x \pm s$). Independent-samples t tests were used for two-group comparisons between MRL/lpr and age-matched C57BL/6 mice at each time point, including 24-hour urinary protein, serum ANA and dsDNA concentrations, serum and urinary GSK-3β and NF-κB p65 concentrations, and renal gene expression, whereas one-way ANOVA followed by the LSD post hoc test was used for comparisons of 24-hour urinary protein, serum ANA and dsDNA concentrations, renal gene and protein expression, and immunohistochemical scores among the C57, LN, and CTX groups. A two-sided p value below 0.05 was considered statistically significant. Analyses were conducted in SPSS version 26.0. Statistical tests were selected according to the number of groups being compared, and p values are reported

Table 1. Sequences of upstream and downstream primers for GSK-3β, NF-κB p65, and the internal reference

Gene	Upstream Sequence	Downstream Sequence
Gsk 3β	5'TTCTCGGTACTACAGGGCACCA 3'	5'GTCCTAGCAACAATTCAGCCAACA 3'
NF-κB p65	5'GAAGAACAAGAAATCCTACCCACA 3'	5'GGTCAGAATGCACCAGAAGTCC 3'
GAPDH	5'TGTGTCCGTCGTGGATCTGA 3'	5'TTGCTGTTGAAGTCGCAGGAG3'

Table 2. Levels of 24-hour urinary protein and serum autoantibodies in LN group mice and C57 group mice at various weeks of age

	Group	12W	16W	20W	24W	28W
24-hour urine protein (mg)	LN	0.63±0.16	1.43±0.29**	2.39±1.02*	1.99±0.70*	2.13±0.94*
	C57	0.61±0.06	0.73±0.16	0.73±0.28	0.73±0.15	0.75±0.08
T		0.316	4.771	2.406	3.512	3.935
P		0.760	0.001	0.020	0.014	0.011
ANA (pg/ml)	LN	20.52±1.65	20.73±1.00*	23.05±2.77*	25.00±0.84***	25.14±1.17***
	C57	18.90±0.56	19.14±0.52	18.64±0.16	18.84±0.47	19.05±0.68
T		1.957	3.155	3.555	14.284	10.460
P		0.086	0.013	0.023	< 0.001	< 0.001
dsDNA (ng/ml)	LN	279.38±10.27**	291.45±21.98**	279.95±13.12**	290.53±10.44***	291.56±18.95***
	C57	230.98±18.36	237.76±12.99	236.95±16.97	236.15±8.69	235.00±11.75
T		5.144	4.702	4.482	8.952	5.596
P		0.001	0.002	0.002	< 0.001	< 0.001

Note: *$P < 0.05$, **$P < 0.01$, ***$P < 0.001$. Independent-samples t-tests were utilized to compare the two groups.

with the corresponding results and figure or table where applicable.

Results

Time gradient

Age-related changes in urinary protein and circulating autoantibodies in MRL/lpr mice: From 16 to 28 weeks of age, the LN group showed higher 24-hour urinary protein excretion and serum ANA concentrations than the C57 group ($P < 0.05$). Serum dsDNA concentrations were higher in the LN group than in age-matched C57BL/6 controls at all assessed ages ($P < 0.01$; **Table 2**).

Renal morphology and immune-complex deposition during LN progression: Renal sections from LN mice displayed lesions compatible with type III and type IV LN. The principal features were mesangial cell and matrix expansion, mesangial immune-complex accumulation, crescent formation, focal tubular atrophy, interstitial inflammatory-cell infiltration, and mild thickening of small arterial walls (**Figure 1**). Together, these alterations documented glomerular, tubular, interstitial, and vascular involvement in the LN group.

Immunofluorescence detected granular and lumpy deposits of IgA, IgG, IgM, C1q, and C3 in mesangial regions and along glomerular capillary walls of LN mice. The strongest renal immune-complex signal was observed at 28 weeks (**Figure 2**). The distribution and time-dependent increase in these deposits complemented the structural changes seen on routine histological staining.

Renal GSK-3β and NF-κB p65 expression across the age series: Serum and urinary concentrations of GSK-3β and NF-κB p65 were numerically higher in LN than in C57 mice, but these differences were not statistically significant ($P > 0.05$; **Figure 3A**, **3D**). In contrast, serum NF-κB p65 concentrations were significantly higher in LN mice at 16 weeks ($P < 0.05$; **Figure 3B**), while urinary GSK-3β concentrations were significantly higher at 12 weeks ($P < 0.01$) and 28 weeks ($P < 0.05$; **Figure 3C**).

By contrast, renal gene expression of GSK-3β and NF-κB p65 was elevated in the LN group throughout the 12- to 28-week observation period ($P < 0.01$; **Figure 3E**, **3F**). These renal measurements provided a clearer group difference than the corresponding serum and urine concentrations.

Pharmacological intervention

CTX-associated changes in urinary protein and autoantibodies: After CTX treatment, 24-hour

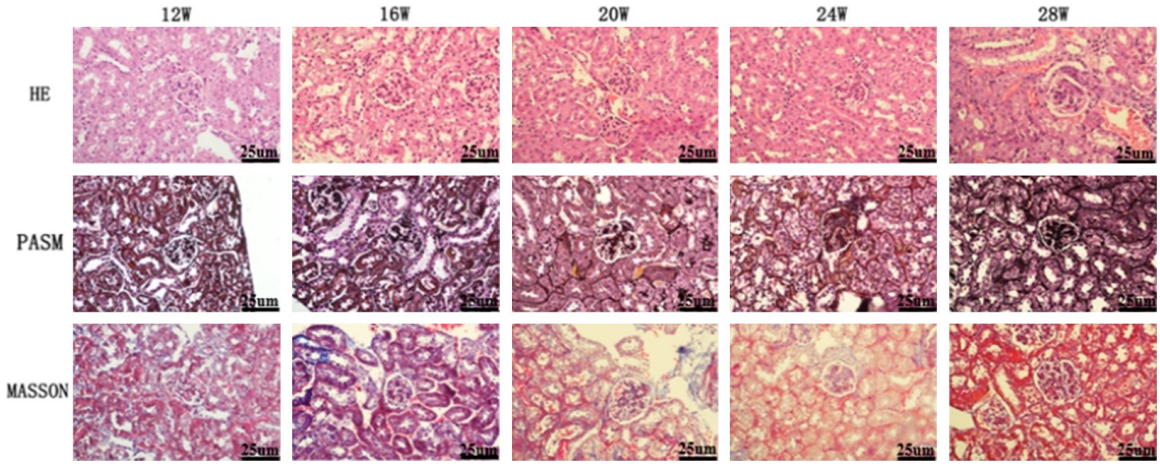


Figure 1. Pathological image of the kidney in LN group mice (×40).

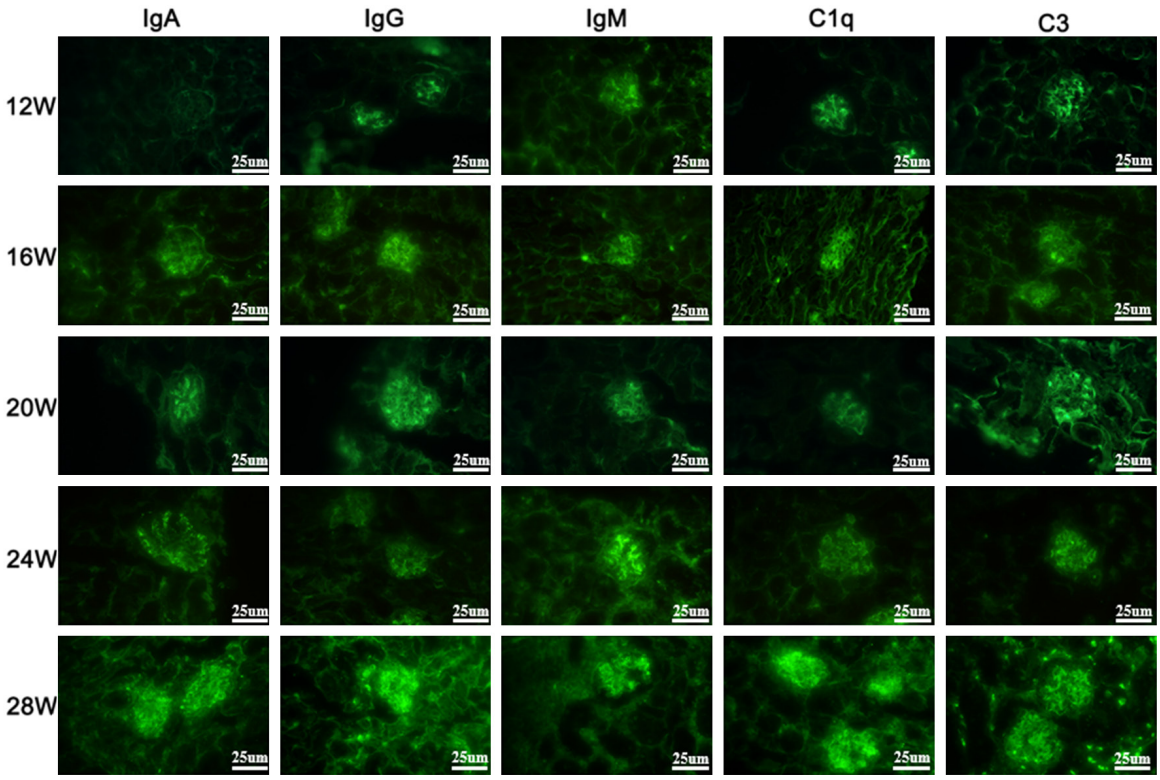


Figure 2. Immunofluorescence image of the kidney in the LN group mice (×40).

urinary protein excretion was lower than in untreated LN mice, although the difference was not significant ($P > 0.05$; **Table 3**). In contrast, serum ANA and dsDNA concentrations were significantly lower in the CTX group than in the untreated LN group, and the overall differences among the three groups were significant for both measures ($P < 0.001$; **Table 3**). Thus, the intervention produced a measurable serological effect even though the urinary-protein result did not meet the significance threshold.

CTX attenuated renal pathological and immunofluorescence abnormalities: Compared with untreated LN mice, CTX-treated mice had less glomerular-cell proliferation and less vacuolar degeneration of renal tubular epithelial cells. No obvious differences in segmental lesions,

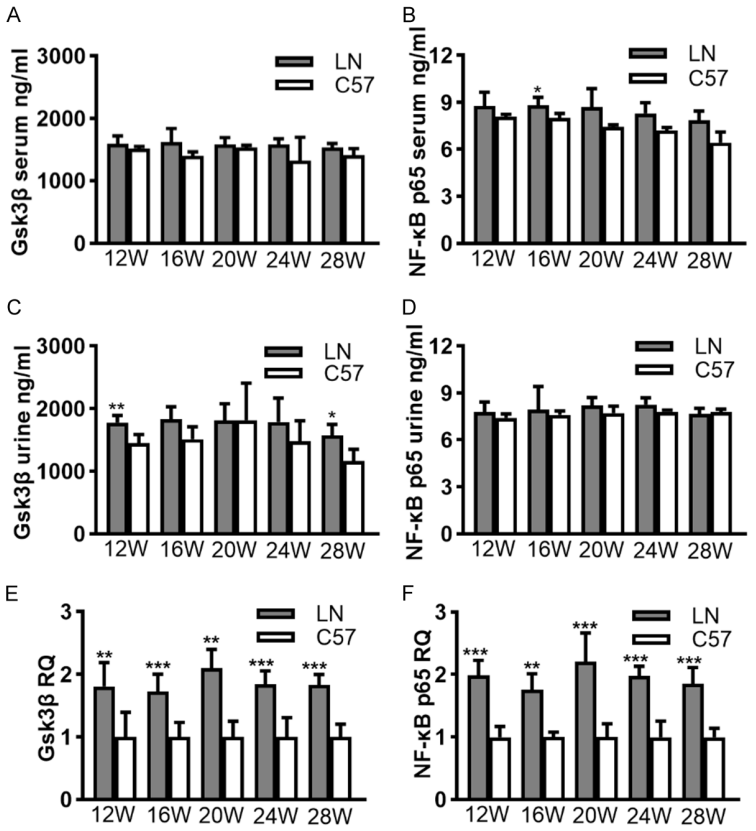


Figure 3. Expression levels of GSK-3β and NF-κB p65 in serum, urine, and kidneys of mice at various weeks of age. *$P < 0.05$, **$P < 0.01$, ***$P < 0.001$. Independent-samples t tests were used to compare MRL/lpr mice with age-matched C57BL/6 mice at each time point.

Table 3. Levels of 24-hour urinary protein and serum autoantibodies in each drug intervention group

Group	24-hour urine protein (mg)	ANA (pg/ml)	dsDNA (ng/ml)
CTX	1.12±1.23	21.44±0.45###	191.63±8.49###
LN	2.13±1.46*	23.99±0.61***	249.48±7.69***
C57	0.75±0.08	21.40±0.77	216.03±6.22
F	3.173	28.378	74.420
P	0.078	< 0.001	< 0.001

Note: * compared with C57, # compared with the LN group; */#$P < 0.05$, **/##$P < 0.01$, ***/###$P < 0.001$. For comparisons involving multiple groups, one-way analysis of variance (ANOVA) followed by the LSD post hoc test was employed.

interstitial fibrosis, inflammatory-cell infiltration, or vascular lesions were observed between the groups (**Figure 4**). Renal immunofluorescence for IgA, IgG, IgM, C1q, and C3 was also weaker after CTX treatment (**Figure 5**). The combined morphological and fluorescence findings indicate attenuation of several renal abnormalities rather than uniform resolution of every pathological feature.

CTX reduced renal GSK-3β and NF-κB p65 expression: Renal GSK-3β and NF-κB p65 gene and protein expression levels were lower in CTX-treated mice than in untreated LN mice ($P < 0.01$; **Figure 6A-E**). Comparisons across all experimental groups were also significant. Immunostaining patterns were evaluated in parallel to determine whether the molecular measurements were accompanied by changes in their renal distribution.

In C57 kidneys, GSK-3β and NF-κB p65 staining was mainly limited to tubular epithelial-cell cytoplasm and membranes. In the LN kidneys, staining was broader, with involvement of both glomeruli and the renal interstitium, and was strongest within the glomeruli. In kidneys from CTX-treated mice, glomerular staining was lighter and the overall signal was lower ($P < 0.05$; **Figures 7**, **8**) compared with untreated LN kidneys. The alterations at the tissue level were consistent with decreased renal gene and protein expression in the CTX group.

Discussion

With advances in LN management, SLE still accounts for a substantial burden of morbidity and mortality. Although we have a more complete understanding of disease mechanisms, that progress has not consistently translated into better therapeutic outcomes. Routine urine testing still provides valuable information, but additional markers are required to identify renal involvement earlier, assess disease activity, and monitor therapeutic response. Such markers may allow a shift toward earlier and more individualized management of lupus-related renal injury. In this context, renal signaling molecules interpreted in conjunction with proteinuria, autoantibodies,

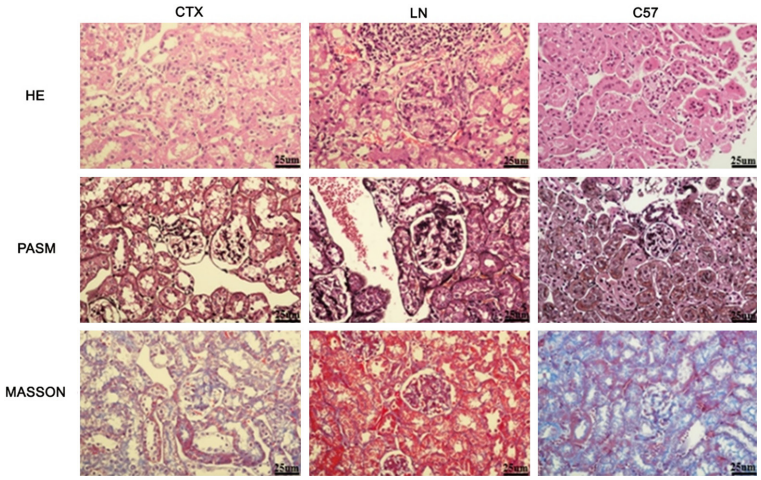


Figure 4. Renal pathology of mice in each group with drug intervention (×40).

and histopathological findings may be more clinically useful than their interpretation in isolation. This is of particular importance in animal studies, where measures can be taken at serological, tissue, and molecular levels at the same time point. Because LN has heterogeneous renal manifestations, no single index can sufficiently represent this disease; therefore, molecular findings must be viewed in the context of the other outcome measures obtained in parallel from the same animals.

The findings as currently reported are biologically plausible, since GSK-3β and NF-κB p65 participate in interconnected inflammatory pathways. GSK-3β can influence NF-κB activity through the nuclear balance of the two transcription factors, p65 and CREB, and their shared coactivator CBP [11, 12]. This is also the case for the NF-κB signaling system, which regulates cytokine transcription, immune activation, and mesangial-cell proliferation in renal disease [13]. In LN models, NF-κB p65 nuclear translocation is linked to inflammatory targets including IL-1, IL-6, and TNF-α [14, 15], whereas reducing NF-κB activity may limit renal inflammatory injury [16, 17]. These observations justify investigating GSK-3β and p65 in parallel but are consistent with the view that the two measurements must be interpreted as part of a larger, cell- and stage-dependent inflammatory network rather than as independent determinants of disease. The findings from the present model provided important information, with serum and urine measurements provided a peripheral view of the disease process, while RT-qPCR, Western blotting, and immunostaining were more directly linked with the renal compartment. These measures can thus corroborate and strengthen the characterization of a phenotype; however, no temporal ordering among signaling events can presently be derived. This distinction is particularly important for GSK-3β and p65, both of which have roles in multiple pathways outside the kidney. Nevertheless, their expression in the kidney may still offer a way to describe the molecular context in which structural and immunological abnormalities arise.

Renal involvement in MRL/lpr mice begins at 12 weeks of age as measured by autoantibody levels, urinary protein excretion, histological injury, and renal immune-complex deposition. This is in line with previous work, as the pattern does not worsen at exactly the same rate across all measures [18]. Proteinuria is present along with perivascular inflammatory-cell infiltration and necrotic change at 16 weeks, supporting the selection of week 16 as the CTX intervention point [19]. It also provided an opportunity to initiate a 12-week treatment period before tissue collection. Using this mouse model, simultaneous evaluation of serological, histological, and molecular changes can be performed, albeit not all clinical features of human LN are reproduced. The selection of the intervention point was thus based on the co-occurrence of serological, urinary, and tissue evidence, rather than on a single readout. It enabled the treated and untreated LN groups to be evaluated at the same terminal age, limiting age-related variation when renal molecular findings were compared.

Renal GSK-3β and NF-κB p65 expression was increased in LN mice between 12 and 28 weeks, and the distribution of immunostaining extended from tubular epithelial compartments in C57 kidneys to glomerular and interstitial regions in LN kidneys. This correspondence supports an association with the renal inflam-

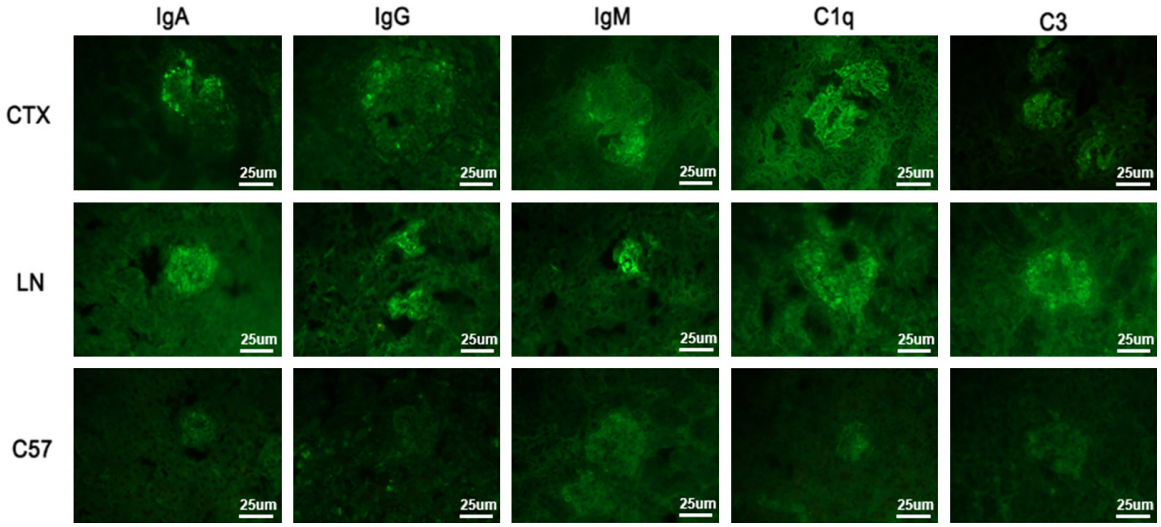


Figure 5. Renal immunofluorescence of mice in each group after drug intervention (×40).

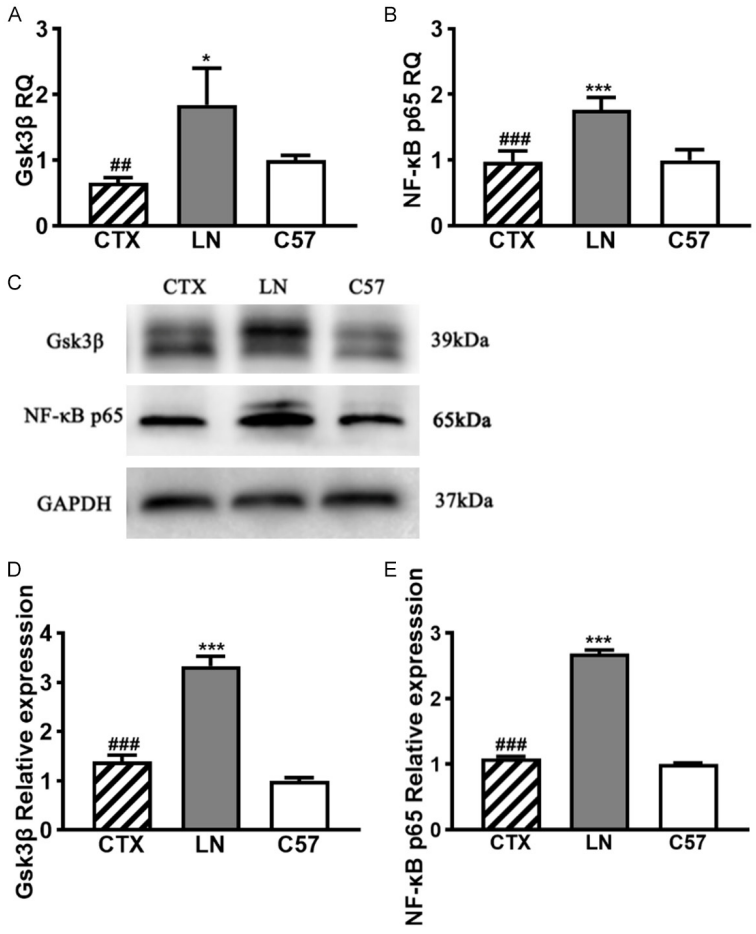


Figure 6. Effects of CTX treatment on renal GSK-3β and NF-κB p65 expression. *Compared with the C57 group; #compared with the LN group; */#$P < 0.05$, **/##$P < 0.01$, ***/###$P < 0.001$. Comparisons among the three groups were performed using one-way analysis of variance (ANOVA) followed by the LSD post hoc test.

matory phenotype, not a demonstration that either molecule initiates injury. Related studies report that GSK-3β inhibition can strengthen Treg-cell suppressive function [20] and can reduce proteinuria, renal inflammation, dsDNA, IgG/C3 deposition, and pro-inflammatory cytokines in MRL/lpr mice [21]. NF-κB dysregulation is similarly implicated in lupus-like autoimmunity and experimental glomerular injury [17, 22]. Because no pathway-blockade experiment was included, the present expression changes should be regarded as correlates of the LN phenotype. The broader distribution of renal staining in LN mice is also consistent with the histological evidence of glomerular and interstitial involvement. However, tissue localization alone cannot identify the cell population in which a signaling change began or determine whether it preceded structural injury. Experiments that combine cell-specific analysis with selective pathway modulation will be required to address those questions.

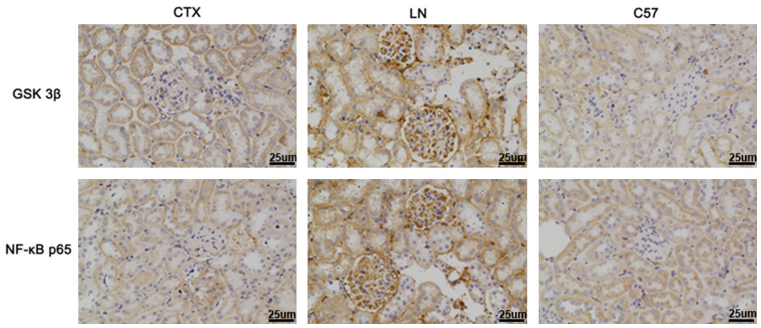


Figure 7. Protein expression of signaling proteins GSK-3β and NF-κB p65 in different regions of the kidney in mice from various drug intervention groups (×40).

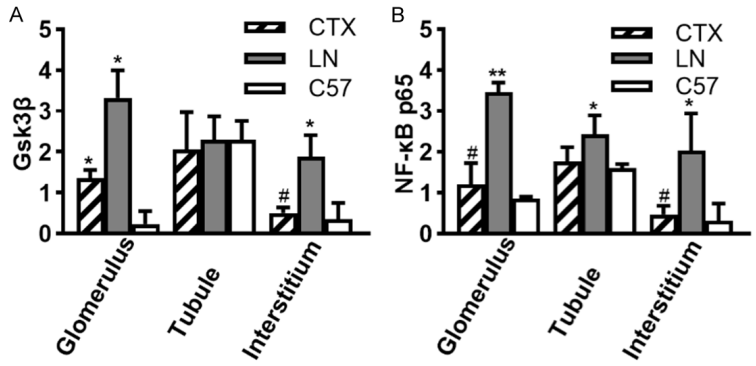


Figure 8. Protein expression levels of GSK-3β and NF-κB p65 in different regions of the kidney in mice from various drug intervention groups. Asterisks indicate comparisons with the C57 group, and number signs indicate comparisons with the LN group. One asterisk or one number sign indicates $P < 0.05$, and two asterisks indicate $P < 0.01$. Comparisons among the three groups were performed using one-way analysis of variance (ANOVA) followed by the LSD post hoc test.

Within the treatment schedule used here, CTX was associated with lower ANA and dsDNA concentrations, milder renal pathological and immunofluorescence abnormalities, and reduced renal GSK-3β and NF-κB p65 expression. The absence of a significant change in 24-hour urinary protein underscores that serological, tissue, and molecular outcomes need to be interpreted together. CTX has an established role in active LN [23], and previous reports describe treatment-related changes in immune and inflammatory markers [24-26]. Similar findings with GSK-3β inhibitors and artemisinin derivatives also support further investigation of these inflammatory pathways in experimental disease [27-31]. However, the observed decrease in GSK-3β and p65 identifies them only as CTX-responsive markers in this model. However, no direct mechanistic role can be assigned until selective inhibition, rescue experiments, and time-resolved tissue studies are performed. In particular, the pattern of lower autoantibody concentrations and weaker renal immune-complex staining after CTX is compatible with a less active inflammatory state, but does not distinguish an upstream action on immune activation from a downstream response to reduced renal injury. The current data therefore support a mechanistic hypothesis for future testing rather than a definitive pharmacological mechanism. Comparing multiple outcome domains was particularly important here because treatment effects were not identical across serological, urinary, morphological, and molecular endpoints.

Taken together, the data show that renal GSK-3β and NF-κB p65 upregulation accompanies LN development in MRL/lpr mice and that CTX treatment coincides with lower expression of both markers and improved renal findings. They support further mechanistic investigation of this inflammatory axis, but they neither validate a clinical biomarker nor establish a direct therapeutic target. Confirmation will require additional models and appropriately designed clinical studies. Future work should also relate molecular changes to repeated functional renal measures and establish whether the same expression pattern is retained across disease stages. Such work would help determine the scope and translational relevance of the association observed in this mouse model.

Conclusion

In contrast, increased levels of renal GSK-3β and NF-κB p65 expression were found during LN progression, whereas decreased expression of both proteins was found after CTX treat-

ment in MRL/lpr mice. Our results also suggest that the CTX response is associated with GSK-3β/NF-κB-related inflammatory signaling; however, this association does not establish causality. Pathway-specific studies are required to determine whether this signaling axis directly mediates renal protection. Accordingly, these data provide a basis for targeted mechanistic experiments, rather than evidence for an immediate clinical application. The conclusions are restricted to the MRL/lpr model and the observation schedule used in this experiment.

Acknowledgements

The authors thank the staff of the College Laboratory Department at Gansu Provincial People's Hospital for their support. This work was supported by the Gansu Province Health Industry Scientific Research Program (GSWSKY2017-35), the Gansu Provincial Natural Science Foundation (21JR1RA035), and the General Project of the Joint Scientific Research Fund of the Gansu Province Science and Technology Plan (23JRRA1539).

Disclosure of conflict of interest

None.

Address correspondence to: Haoling Zhang, Department of Biomedical Science, Universiti Sains Malaysia, Pinang 13200, Malaysia. E-mail: zhanghaolingedu@163.com; Shuhong Zhou, Department of Immunology and Rheumatology, Gansu Provincial Hospital, Lanzhou 730000, Gansu, China. E-mail: zshlz1973@126.com

References

[1] Hoi A, Igel T, Mok CC and Arnaud L. Systemic lupus erythematosus. Lancet 2024; 403: 2326-2338.

[2] Siegel CH and Sammaritano LR. Systemic lupus erythematosus: a review. JAMA 2024; 331: 1480-1491.

[3] Parodis I, Rovin BH, Tektonidou MG, Anders HJ, Malvar A, Mok CC and Mohan C. Lupus nephritis. Nat Rev Dis Primers 2025; 11: 69.

[4] Obrișcă B, Jurubiță R, Andronesi A, Sorohan B, Achim C, Bobeica R, Gherghiceanu M, Mandache E and Ismail G. Histological predictors of renal outcome in lupus nephritis: the importance of tubulointerstitial lesions and scoring of glomerular lesions. Lupus 2018; 27: 1455-1463.

[5] Zhang F, Zhang B, Tang R, Jiang H, Ji Z, Chen Y and Feng H. The occurrence of lupus nephritis is regulated by USP7-mediated JMJD3 stabilization. Immunol Lett 2021; 235: 41-50.

[6] Turkistani A, Al-Kuraishy HM, Al-Gareeb AI, Albuhadily AK, Alexiou A, Papadakis M, Elfiky MM, Saad HM and Batiha GE. Therapeutic potential effect of glycogen synthase kinase 3 beta (GSK-3β) inhibitors in Parkinson disease: exploring an overlooked avenue. Mol Neurobiol 2024; 61: 7092-7108.

[7] Han D, Medina-Rodriguez EM, Lowell JA and Beurel E. Glycogen synthase kinase-3 promotes T helper type 17 differentiation by promoting interleukin-9 production. Immunology 2020; 160: 357-365.

[8] Zou MS, Song QJ, Yin TY, Xu HT and Nie GM. Vitamin D activates miR-126a-5p to target GSK-3β and alleviates systemic lupus erythematosus in MRL/LPR mice. Curr Pharm Biotechnol 2023; 24: 1803-1811.

[9] Cimé-Aké E, Barrera-Vargas A, Demichelis-Gómez R, Ramírez-Alemón M and Rull-Gabayet M. Description of therapeutic strategies in severe systemic lupus erythematosus-associated immune thrombocytopenia: a retrospective cohort study of response and relapse. Clin Rheumatol 2024; 43: 2521-2532.

[10] Zhang Y, Xu Q, Wang Y, Zhang C, Xu S, Luo M and Yang S. Caragana sinica (Buc'hoz) Rehd. (jin ji er) polysaccharide regulates the immune function and intestinal microbiota of cyclophosphamide (CTX) induced immunosuppressed mice. J Ethnopharmacol 2024; 322: 117551.

[11] Sabeel Z, Wang J, Dong J, Liu Y, Yu C and Yang Z. The duality of GSK-3β in urinary bladder cancer: tumor suppressor and promoter roles through multiple signaling pathways. Biochim Biophys Acta Rev Cancer 2025; 1880: 189324.

[12] Ahmed MA, Kamel EO and Abd-Eldayem AM. Role of cAMP/pCREB and GSK-3β/NF-κB p65 signaling pathways in the renoprotective effect of mirabegron against renal ischemia-reperfusion injury in rats. Eur J Pharmacol 2024; 974: 176617.

[13] Ren N, Wang WF, Zou L, Zhao YL, Miao H and Zhao YY. The nuclear factor kappa B signaling pathway is a master regulator of renal fibrosis. Front Pharmacol 2024; 14: 1335094.

[14] Shoctor NA, Brady MP, Lightman RR, Overton KN, Tandon S, Mathis SP, Rane MJ, Barati MT, Arriens CG, Powell DW and Caster DJ. Serum NF-κB-regulated biomarkers of proliferative lupus nephritis. Glomerular Dis 2025; 5: 328-343.

[15] Li J, Wang L, Zeng G, Li H, Luo J, Tian Q and Zhang Z. Chymotrypsin attenuates adjuvant-

induced arthritis by downregulating TLR4, NF-κB, MMP-1, TNF-α, IL-1β, and IL-6 expression in Sprague-Dawley rats. Immunopharmacol Immunotoxicol 2022; 44: 959-969.
[16] Liu Y, Yu C, Ji K, Wang X, Li X, Xie H, Wang Y, Huang Y, Qi D and Fan H. Quercetin reduces TNF-α-induced mesangial cell proliferation and inhibits PTX3 production: involvement of NF-κB signaling pathway. Phytother Res 2019; 33: 2401-2408.
[17] Caster DJ and Powell DW. Precision targeting of NF-κB signaling in lupus nephritis. Lupus (Los Angel) 2020; 6: 160.
[18] Shi Y, Yao W, Sun L, Li G, Liu H, Ding P, Hu W and Xu H. The new complement inhibitor CRIg/FH ameliorates lupus nephritis in lupus-prone MRL/lpr mice. BMC Nephrol 2019; 20: 424.
[19] Halkom A, Wu H and Lu Q. Contribution of mouse models in our understanding of lupus. Int Rev Immunol 2020; 39: 174-187.
[20] Cheng H, Wang L, Yang B, Li D, Wang X, Liu X, Tian N, Huang Q, Feng R, Wang Z, Liang R, Dai SM, Lv L, Wu J, Zang YS and Li B. Cutting edge: inhibition of glycogen synthase kinase 3 activity induces the generation and enhanced suppressive function of human IL-10(+) FOXP3(+)-induced regulatory T cells. J Immunol 2020; 205: 1497-1502.
[21] Zhao J, Wang H, Huang Y, Zhang H, Wang S, Gaskin F, Yang N and Fu SM. Lupus nephritis: glycogen synthase kinase 3β promotion of renal damage through activation of the NLRP3 inflammasome in lupus-prone mice. Arthritis Rheumatol 2015; 67: 1036-1044.
[22] Brady MP, Korte EA, Caster DJ and Powell DW. TNIP1/ABIN1 and lupus nephritis: review. Lupus Sci Med 2020; 7: e000437.
[23] Prasad N, Kurian J, Agarwal V, Bhadauria D, Behera M, Yacha M, Kushwaha R, Agrawal V, Jain M and Gupta A. Long-term outcomes of lupus nephritis treated with regimens based on cyclophosphamide and mycophenolate mofetil. Lupus 2020; 29: 845-853.
[24] Yang X, Liang J, Shu Y, Wei L, Wen C, Luo H, Ma L, Qin T, Wang B, Zeng S, Liu Y and Zhou C. Asperosaponin VI facilitates the regeneration of skeletal muscle injury by suppressing GSK-3β-mediated cell apoptosis. J Cell Biochem 2024; 125: 115-126.
[25] Yao J, Liu J, He Y, Liu L, Xu Z, Lin X, Liu N and Kai G. Systems pharmacology reveals the mechanism of Astragaloside IV in improving immune activity on cyclophosphamide-induced immunosuppressed mice. J Ethnopharmacol 2023; 313: 116533.
[26] Zhou QS, Hu J and Hu H. Analysis of changes in joint function and peripheral blood mononuclear cells in patients with systemic lupus erythematosus and intervention effects of different drugs. Eur Rev Med Pharmacol Sci 2017; 21: 4423-4430.
[27] Wang T, Zhang J, Wei H, Wang X, Xie M, Jiang Y and Zhou J. Matrine-induced nephrotoxicity via GSK-3β/nrf2-mediated mitochondria-dependent apoptosis. Chem Biol Interact 2023; 378: 110492.
[28] Liu Q, Kong Y, Guo X, Liang B, Xie H, Hu S, Han M, Zhao X, Feng P, Lyu Q, Dong W, Liang X, Wang W and Li C. GSK-3β inhibitor TDZD-8 prevents reduction of aquaporin-1 expression via activating autophagy under renal ischemia reperfusion injury. FASEB J 2021; 35: e21809.
[29] Hart DA. Sex-specific effects of LiCl treatment on preservation of renal function and extended life-span in murine models of SLE: perspective on insights into the potential basis for survivorship in NZB/W female mice. Biol Sex Differ 2016; 7: 31.
[30] Efferth T and Oesch F. The immunosuppressive activity of artemisinin-type drugs towards inflammatory and autoimmune diseases. Med Res Rev 2021; 41: 3023-3061.
[31] Diao L, Li M, Tao J, Xu X, Wang Y and Hu Y. Therapeutic effects of cationic liposomes on lupus-prone MRL/lpr mice are mediated via inhibition of TLR4-triggered B-cell activation. Nanomedicine 2022; 40: 102491.